Complex Growth of NanoAu on BN Nanomeshes Supported by Ru(0001)

ARTICLE *in* THE JOURNAL OF PHYSICAL CHEMISTRY C · MAY 2008

Impact Factor: 4.77 · DOI: 10.1021/jp7119608

3 AUTHORS, INCLUDING:

Yunbin He
Hubei University
80 PUBLICATIONS **1,191** CITATIONS
SEE PROFILE

Herbert Over
Justus-Liebig-Universität Gießen
196 PUBLICATIONS **5,903** CITATIONS
SEE PROFILE

Article

Complex Growth of NanoAu on BN Nanomeshes Supported by Ru(0001)

A. Goriachko, Y. B. He, and H. Over

J. Phys. Chem. C, **2008**, 112 (22), 8147-8152• DOI: 10.1021/jp7119608 • Publication Date (Web): 13 May 2008

ARTICLES

Complex Growth of NanoAu on BN Nanomeshes Supported by Ru(0001)

A. Goriachko, Y. B. He, and H. Over*

Department of Physical Chemistry, Justus-Liebig-University, Heinrich-Buff-Ring 58, D-35392 Gießen, Germany

Received: December 20, 2007; Revised Manuscript Received: February 28, 2008

Detailed scanning tunneling microscopy measurements reveal the complex interaction of Au with a h-BN nanomesh on Ru(0001). The h-BN overlayer on Ru(0001) consists essentially of a hexagonal lattice of 2 nm wide pores with an in-plane lattice constant of 3.25 nm. The h-BN nanomesh can be regarded as a highly regular network of trapping sites in which Au particles have shown to condense exclusively with a narrow size distribution, thus forming well-suited Au model catalysts. At higher Au coverages two-dimensional metal islands are formed on as well as under the h-BN nanomesh depending on the deposition and annealing procedure. Au atoms can penetrate through defects in the h-BN nanomesh (most notably at step edges) in between the h-BN nanomesh and the Ru(0001) substrate at higher temperatures (activates process). Multi layers of Au form a continuous film between Ru(0001) and h-BN after annealing to 1050 K, thereby lifting the nanostructuring of the h-BN layer due to the weak interaction of h-BN with Au.

1. Introduction

Gold has attracted much scientific attention over the past two decades which was triggered by the pioneering work of Haruta and co-workers, manifesting tremendous differences in the catalytic activity between bulk Au and Au nanoparticles.[1] Not only supported Au nanoparticles but also nanoconfinement of gold in just one dimension is sufficient for the high catalytic activity of Au to appear.[2]

One way to produce supported Au nanoparticles is simply evaporating Au atoms in ultrahigh vacuum (UHV) onto widely used metal oxide substrates.[3,4] A more elaborate method to fabricate supported Au clusters with a very narrow size distribution is the mass selective deposition of preformed Au clusters onto various substrate surfaces.[5] However, supported Au catalysts are facing a major problem with the sintering of the Au nanoparticles under typical reaction conditions.[6] For the case of $TiO_2(110)$, oxygen vacancies[3] or oxidized (alkaline) $TiO_2(110)$[7] may provide nucleation sites for anchoring the Au clusters, thereby impeding a sintering of the Au clusters up to 500 K.[8]

The recently discovered nanomesh of hexagonal BN (h-BN) on Rh(111)[9] and on Ru(0001)[10] has been considered as a promising oxygen-free template for supporting Au nanoparticles. The h-BN nanomesh on Rh(111) and on Ru(0001) consists essentially of a regular hexagonal structure of 2 nm wide pores in the h-BN layer with an in-plane lattice constant of 3.25 nm. The h-BN nanomesh can be viewed as a highly regular network of trapping sites in which deposited Au atoms may preferentially condense into Au nano particles with maximum size determined by the pore size. The corrugation of the h-BN nanomesh may hamper sintering of the Au particles.

In this paper, we present a detailed scanning tunneling microscopy (STM) study, exploring the complex interaction of Au with a h-BN nanomesh on Ru(0001). These measurements are supported by analytic techniques such as Auger electron spectroscopy (AES) and X-ray photoelectron spectroscopy (XPS). Besides Au particles with a narrow size distribution two-dimensional Au islands are identified on h-BN/Ru(0001) by depositing Au at room temperature (RT). A subsequent annealing at 1050 K causes Au islands to intercalate between the h-BN nanomesh and Ru(0001). Multilayers of Au form a continuous film between Ru(0001) and h-BN after annealing to 1050 K, thereby forming a flat and noncorrugated h-BN layer due to the weak interaction of h-BN with Au as compared to Ru.[11]

2. Experimental Details

The experiments were conducted in two separate UHV chambers. Both chambers offer facilities for annealing and ion sputtering of the sample as well as for gold evaporation. One chamber houses STM and XPS; the second chamber was equipped with an Auger electron spectrometer. During substrate preparation the single crystalline Ru(0001) sample was held at 1050 K and cleaned by Ar^+ (1.5 keV) ion sputtering and subsequently annealed in O_2 ($p \approx 2 \times 10^{-7}$ mbar) to remove segregating C contamination via oxidation to CO. To produce the h-BN nanomesh the well-prepared Ru(0001) surface was exposed to $\sim 3 \times 10^{-7}$ mbar of borazine $(BHNH)_3$ for 180 s at a sample temperature of 1050 K. The freshly synthesized high-purity borazine was supplied by H. Sachdev.[12] After the borazine flux was switched off the substrate temperature was still kept at 1050 K for several minutes. This preparation recipe resulted always in a Ru(0001) surface that was completely covered by the h-BN nanomesh. Gold was evaporated onto the h-BN nanomesh with an e-beam evaporator at a rate of 0.1 ML/min. The Au source was calibrated by monitoring the Au (NVV, 69 eV)/Ru (MNN, 273 eV) peaks ratio in AES.

* To whom correspondence should be addressed. E-mail: Herbert.Over@phys.chemie.uni-giessen.de. Fax: +49-641-9934559.

10.1021/jp7119608 CCC: $40.75
Published on Web 05/13/2008

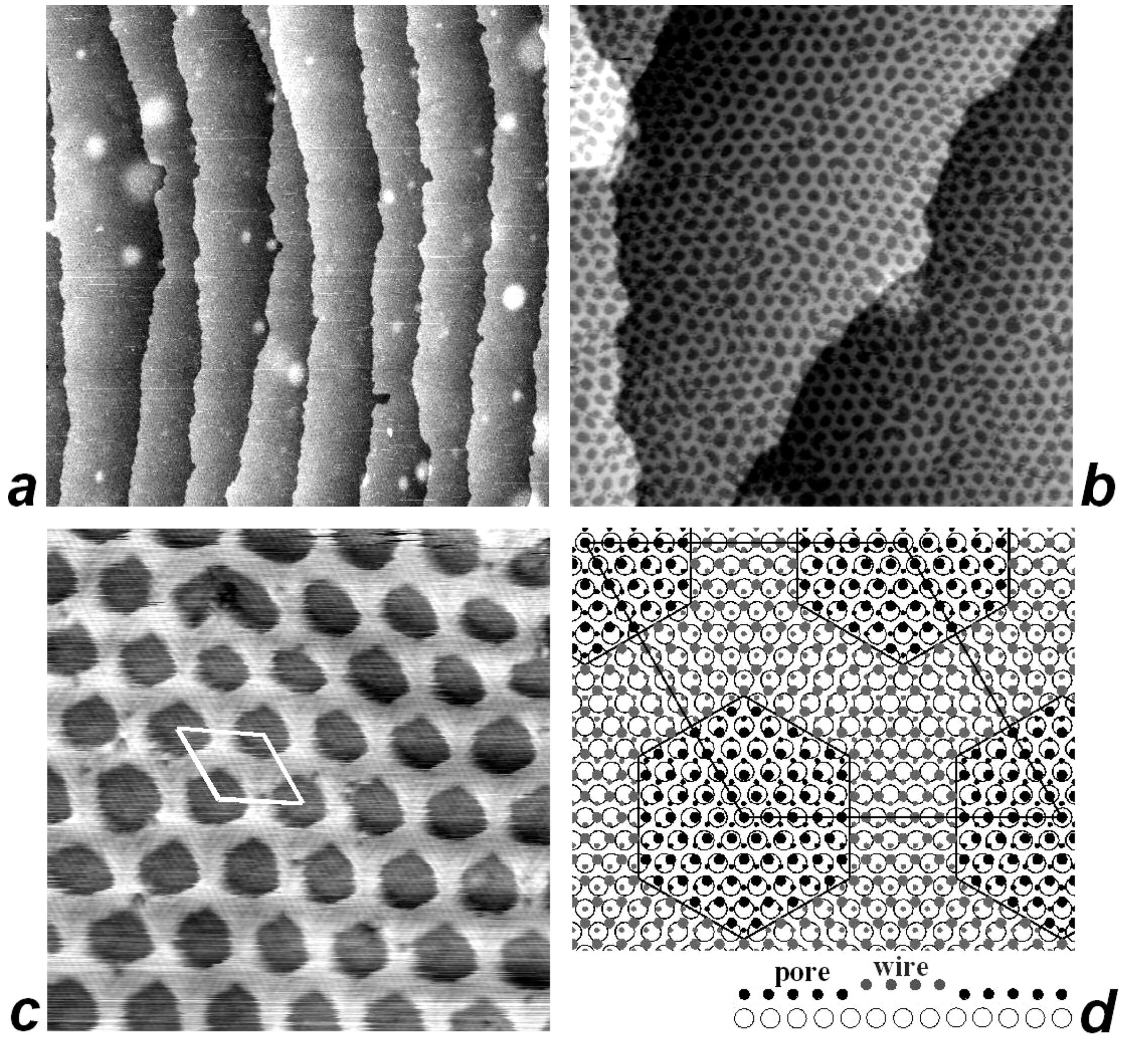

Figure 1. STM image of the pure h-BN/Ru(0001) surface: (a) 431 nm × 431 nm, $U_{sample} = 1$ V, $I_{tunneling} = 1$ pA; large scale image of terraces and steps after typical nanomesh preparation. (b) 86 nm × 86 nm, $U_{sample} = 1.05$ V, $I_{tunneling} = 1$ nA; the nanomesh is a periodic array of darker depressions (pores). (c) 17 nm × 17 nm, $U_{sample} = 0.1$ V, $I_{tunneling} = 8$ nA; high-resolution image demonstrating the hexagonal shape of the pores. The unit cell is indicated. The superimposed lattice of presumably nitrogen atoms is discernible. (d) Top view of the single layer model of h-BN/Ru(0001); large open circles are surface Ru atoms; small filled circles correspond to nitrogen atoms and the dots to boron atoms. The hexagons indicate the boundaries of the pores; dark rhombus designates the unit cell. The side view illustrates the corrugation in the h-BN layer.

3. Results and Discussion

Figure 1a shows a typical large scale image of the h-BN/Ru(0001) surface. The underlying Ru(0001) terraces are atomically flat, except for some round-shaped elevations which originate from the subsurface argon bubbles.[13] A detailed STM analysis reveals that the entire Ru(0001) surface is uniformly covered by the h-BN nanomesh. Figure 1b displays a typical image of the nanomesh, covering neighboring terraces that are separated by single substrate steps. The term "nanomesh" stems from the early observation of a similar structure on the Rh(111) substrate by Corso et al.,[9] when a h-BN double-layer nanomesh model was proposed but later replaced by a corrugated single h-BN layer.[10,14,15] Yet, the appearance of the h-BN layer in STM is suggestive of an apparent nanomesh so that we keep with the term h-BN nanomesh as a kind of "trademark". The h-BN/Ru(0001) reveals in STM a regular network of lower-lying BN regions (dark) and higher-lying BN regions (bright). In the following we will use the term "pore" for the lower BN region and the term "wire" for the upper BN region. The pores of h-BN/Ru(0001) may serve as trapping sites for molecules or clusters. The h-BN nanomesh on Ru(0001) is not strictly periodic, displaying local fluctuations in size, shape, and periodicity of the pores. The average distance between the centers of neighboring pores is 3.25 nm (i.e., 12 unit cells of Ru substrate), and the pore size is 2 nm across.

High-resolution STM image (Figure 1c) of the h-BN/Ru(0001) emphasizes the hexagonal shape of the pores with a superimposed lattice with a periodicity of ∼0.25 nm, both on the wires and in the pores. This value agrees well with the 0.25-nm periodicity within the h-BN basal plane. Very likely only the nitrogen atoms in the h-BN nanomesh are imaged in Figure 1c, as discussed in a previous paper by Berner et al.[16] The selective imaging of nitrogen atoms is related to the higher local density of states (LDOS) near the Fermi level on the nitrogen atoms. The apparent wire/pore height difference of ∼0.1 nm in STM is too small to be compatible with interlayer distance of 0.33 nm in a h-BN double layer. Together with additional experimental and theoretical evidence,[10,11,14–16] a single corrugated h-BN layer model for h-BN/Ru(0001) is clearly favored.

The h-BN basal plane is periodically modulated by the varying strength of interaction of the BN layer with the Ru(0001) substrate surface across the (12 × 12) unit cell (cf. Figure 1d). The interaction of the basal h-BN plane and the Ru(0001) is strongest in those regions where N atoms sit close to on-top

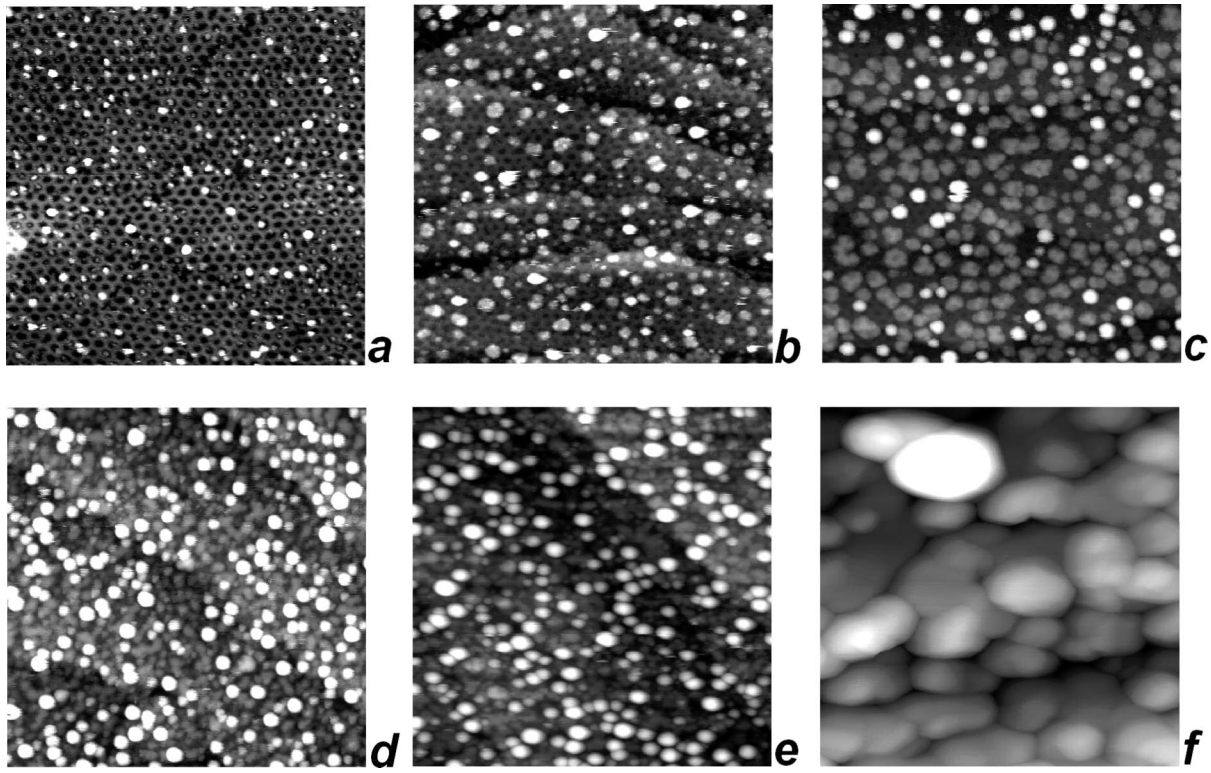

Figure 2. STM images 86 nm × 86 nm of RT grown Au films on h-BN/Ru(0001): (a) Au coverage $\Theta_{Au} = 0.1$ ML, $U_{sample} = 1.15$ V, $I_{tunneling} = 0.6$ nA; (b) 0.2 ML, 1.4 V, 1 pA; (c) 0.3 ML, 1.0 V, 0.5 nA; (d) 0.5 ML, −1.05 V, 5.5 nA; (e) 1 ML, 2.0 V, 1 nA; (f) 14 ML, −1.8 V 1 nA. Depending on the tip condition the clusters were dragged by the STM tip. To overcome this problem, the interaction between the tip and the sample had to be minimized by setting the tunneling current to the lowest possible value of 1 pA and by adjusting the bias voltage.

Ru positions.[15] Therefore the pores of h-BN/Ru(0001) correspond to regions where h-BN is strongly bonded to the Ru(0001) substrate, while the wires of the h-BN nanomesh are attributed to regions with weak cohesion to the Ru(0001) surface. This heterogeneous interaction pattern produces the observed height corrugation of the h-BN nanomesh observed in STM. The wire/pore height corrugation is illustrated in the side view of Figure 1d. The hexagonal borderline between the pores and the wires in Figure 1d is chosen to fit the STM image in Figure 1c. The exact location of the boarderline and hence the exact pore size and wire thickness cannot be determined by STM since various STM images of the nanomesh have displayed varying wire thicknesses. The wires with their weak interaction to the substrate are susceptible to deformations induced by the STM tip, thus masking the true topography of the nanomesh in STM measurements.

During Au deposition the h-BN/Ru(0001) sample was kept at RT. Figure 2 shows STM images of progressively larger amounts of gold deposited on the nanomesh. In Figure 2a, 0.1 ML of gold appears in the form of round nanoparticles with a diameter of up to 2 nm. An important observation is that most of Au particles are sitting in the nanomesh pores. Therefore, at room temperature the deposited Au atoms can readily diffuse across the surface until the Au atoms are trapped in a pore. The pores serve as nucleation sites in which gold nanoparticles grow with a maximum diameter defined by the pore size. The physical reason for the trapping ability of the pores is seen in dipole rings imposed by the pores.[17]

Parts b and c of Figure 2 indicate that a further increase of the Au loading on the h-BN nanomesh at RT (0.2 and 0.3 ML respectively) produces both 2D islands as well as round 3D Au nanoparticles.

The 3D nanoparticles for 0.3 ML Au deposition are substantially larger than a single pore (diameter 3 ± 1 nm). The observed Au islands extend over several nanomesh periods and display the same pore-wire corrugation as the h-BN nanomesh; in the following referred to as Au replica islands. For 0.5 ML of Au (Figure 2d) the islands and particles cover the nanomesh uniformly. An increase of the Au coverage to 1 ML (parts d and e of Figure 2) leads to a higher density of Au particles. A pronounced 3D growth mode is observed for 14 ML Au deposition at room temperature (Figure 2f); the Au film consists of large grains.

In Figure 3a, we show a magnified STM image and a cross-section profile of a Au replica island. The height of the Au islands is ∼0.5 nm, which is consistent with two atomic layers of gold. However, the real height of the replica island can be different from 0.5 nm due to electronic density of states effects in STM. The periphery of the Au replica island is not sharp. The Au replica islands exhibit the same corrugation and pore registry as the surrounding h-BN nanomesh. By assumption that the Au islands are located on the h-BN nanomesh, this finding provides convincing evidence that the apparent pore/wire corrugation of 0.1 nm is the true corrugation, thus corroborating the single layer model.[10,15,16] We should note that a buried Au double layer would equally exhibit the same pore registry as observed in Figure 3a as long as the additional Au layers continue the AB stacking sequence of hcp Ru(0001). An interpretation of the Au replica islands in terms of double layers below the h-BN nanomesh is not convincing as we do not observe with STM any distortions of the h-BN nanomesh at the perimeters of the Au islands. Moreover, thermodynamics would drive the Au double layer into an Au single layer, since the Au−Ru bond is substantially stronger than the Au−Au bond. Buried single Au layers are easy to identify with STM since the pore structure covering these islands should be out of registry with the rest of the h-BN layer, which, however, is not observed in STM. Therefore we strongly favor the assignment of Au

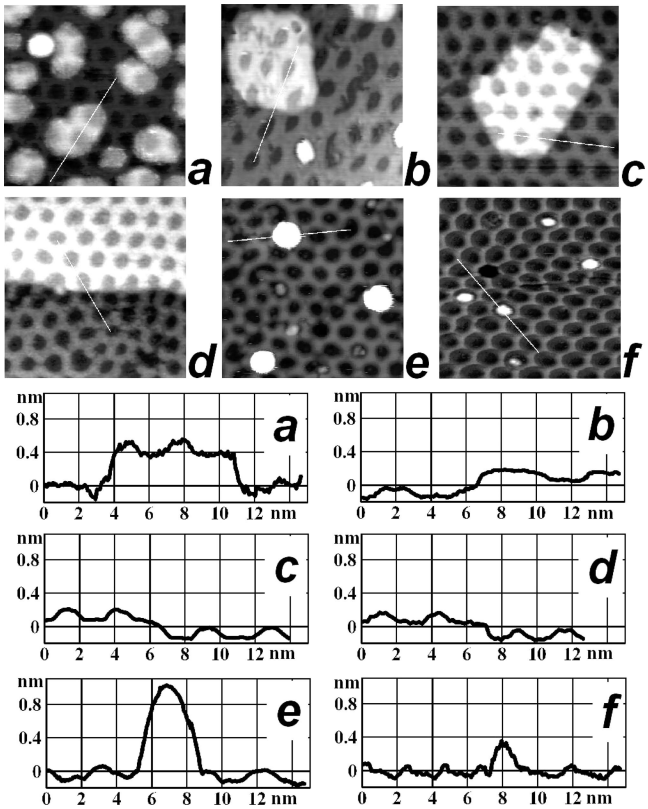

Figure 3. Zoom in STM images and cross-sectional cuts along the indicated white lines: (a) the replica island from Figure 2c. (b) One of the numerous 2D islands appearing after RT deposition of 0.5 ML Au and subsequent annealing at 1050 K. (c) Ru islands below h-BN/Ru(0001). (d) h-BN covering two neighboring terraces separated by a single step. (e) One of the largest round nanoparticles observed after RT deposition of 0.1 ML Au and annealing at 875 K. (f) Round nanoparticles fitting inside the nanomesh aperture after RT deposition of 0.2 ML Au and annealing at 1050 K.

replica islands in Figure 3a to be on-surface Au islands. We should note that Co on the h-BN/Ni(111) intercalates below the h-BN layer even at room temperature.[18]

After deposition of 0.5 ML of Au onto the h-BN/Ru(0001) at RT and annealing the system at 1050 K we could produce single-layer Au islands below the h-BN (Figure 3b). Such islands have similar height and broken registry relative to the surrounding nanomesh, as the single substrate layer islands (Figure 3c), or generally as observed on the neighboring terraces across the step edge (Figure 3d). In parts e and f of Figure 3, we present a detailed view and a cross section through one of the largest (Figure 3e) and one of the smallest (Figure 3f) Au nanoparticles. The larger particle is 4 nm wide and 0.8 nm high. The small Au particle is less than 2nm in diameter and its height is 0.4 nm, fitting perfectly into the h-BN pores. On the basis of the cross-sectional cuts in parts e and f of Figure 3 and the bulk density of gold and by assumption of no shape distortion due to the STM tip geometry, one arrives at an estimation of ~400 (Figure 3e) and ~30 (Figure 3f) Au atoms inside of such Au nanoparticles. Because of a tendency of any real STM tip to overestimate the size of three-dimensional objects, the nanoparticles may consist of lesser atoms than our simple estimate suggests.

In the following we studied the changes of RT-deposited Au films due to annealing at 1050 K for 5 min. Parts a and b of Figure 4 display STM images of these annealing experiments for initial Au coverages of 0.1 and 0.2 ML, respectively. In both cases the annealing procedure results in round Au particles sitting inside the pores. At 0.3 ML of deposited Au (Figure 4c) the annealed surface shows a higher density (than in parts a and b of Figure 4) of Au nanoparticles, which are up to ~5 nm wide and do not fit into the nanomesh pores.

Further increase of Au loading (0.5 ML of Au) does not lead to even larger particles upon 1050 K annealing. Instead islands with lateral dimensions of several nanomesh periods appeared (Figure 4d). The nanomesh periodicity and corrugation on top of each island is similar to the surrounding nanomesh. With 1 ML deposited Au (Figure 4e) and after 1050 K annealing the islands grow in size and number. The nanomesh corrugation is mostly present on top of these islands, yet in some areas the pore structure disappeared. When a large amount of Au (14 ML) was deposited and subsequently annealed at 1050 K (Figure 4f) no pore structure at all is seen in STM. Only some Au nanoparticles are visible on the flat structureless surface.

The apparent height of the islands in Figure 4d is ~0.2 nm above the substrate (a detailed view of one of them is given in Figure 3b), i.e., very close to the 0.21 nm step height of the Ru(0001) substrate (see detailed view in Figure 3d). The surface of this kind of island exposes a structure with ~0.1 nm corrugation (height difference between the wire and the pore), similar to that of the h-BN/Ru(0001) nanomesh. Comparing the pore registries across the peripheries of the islands in parts b and c of Figure 3 with those across the step-edge in Figure 3d, we notice that the registry is broken in all three cases. This observation excludes that the Au islands are on the surface. Otherwise the pore structure on the islands should be in registry with that of the underlying h-BN nanomesh which is experimentally not observed. Therefore we conclude that the BN nanomesh covers the metal islands in parts b and c of Figure 3, i.e., the islands are buried beneath the nanomesh.

According to AES results shown below, there is no loss of Au observed due to annealing, if the initial RT-deposited $\theta_{Au} \geq 0.3$ ML. Instead Au gets buried under the h-BN, either forming an alloy with Ru or a pseudomorphic Au film on the Ru(0001) substrate. As a consequence the resulting surface has a higher atomic step density which is manifested by numerous islands of single-atomic layer. We should recall that Au and Ru do not form a bulk alloy.[19] However, it might be that Au and Ru are able to stabilize a surface alloy such as observed with Au and Ni.[20] Furthermore the interatomic distance must be very similar to that of the underlying Ru(0001) substrate (otherwise the h-BN layer would change the periodicity).

To corroborate the interpretation of the STM data given above, we have performed AES investigations of the Au behavior on the h-BN/Ru(0001) upon deposition at RT and annealing at 1050 K. Figure 5 shows the differentiated AES spectra excited by 3 keV primary electrons and the corresponding chart of peak-to-peak signal ratios: Au (NVV, 69 eV)/Ru ($M_VN_VN_V$, 273 eV) and N (KLL, 379 eV)/Ru ($M_VN_VN_V$, 273 eV). A firm interpretation of the AES peak of B (KLL, 179 eV) suffers from a severe overlap with one of the Ru MNN peaks. A ratio of $Au_{NVV}/Ru_{MNN} = 0.55$ is referred to as 1 ML of gold deposited onto the clean Ru(0001) surface. All spectra clearly demonstrate the absence of any carbon contamination resulting from deposition or annealing procedures. This can be judged by the unchanging relative magnitudes and shapes of the Ru $M_VN_IN_V$ and the Ru $M_VN_VN_V$ peaks, the latter having a severe overlap with the possible C KLL peak. Inspection of the ratios in Figure 5 shows that the gold amount declines (most likely due to evaporation into vacuum) as a result of 1050 K annealing only if the initially deposited Au coverage is smaller

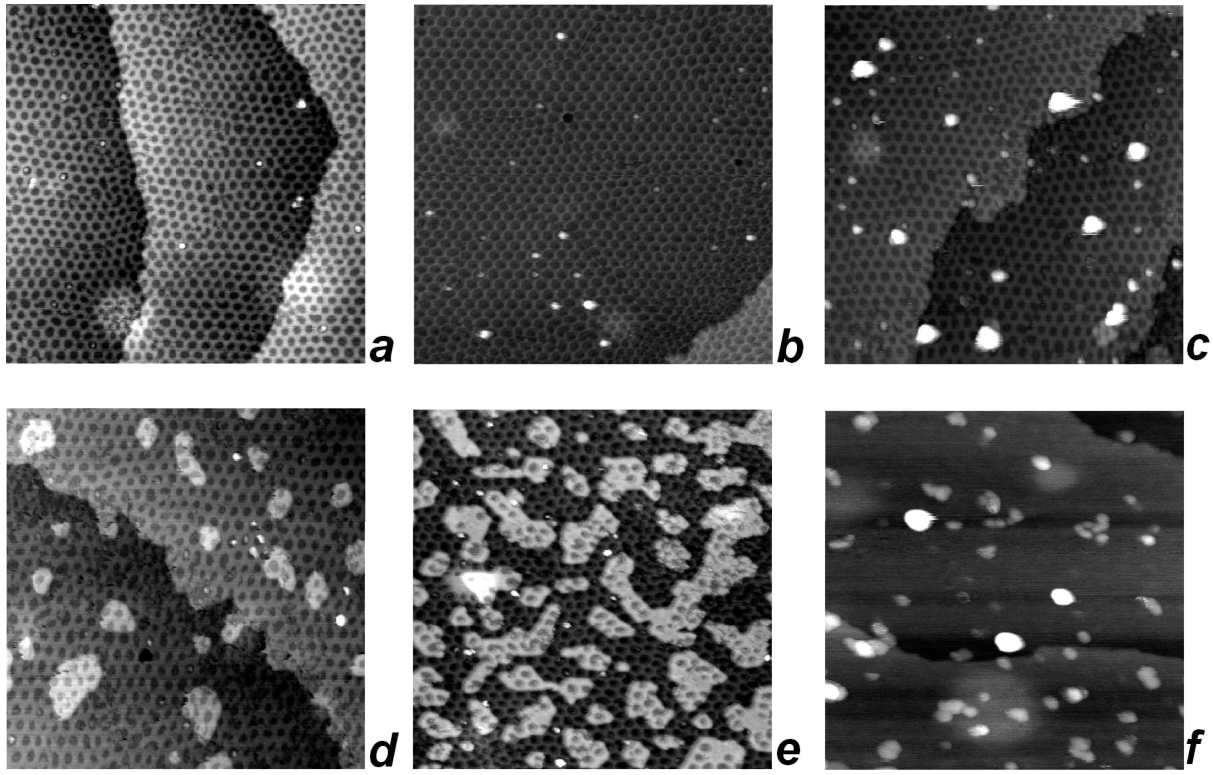

Figure 4. STM images 86 nm × 86 nm after annealing at 1050 K for 5 min, with initially deposited Au on h-BN/Ru(0001): (a) Au coverage $\Theta_{Au} = 0.1$ ML, $U_{sample} = 2.0$ V, $I_{tunneling} = 3$ pA; (b) 0.2 ML, 1.8 V, 1 pA; (c) 0.3 ML, 2.55 V, 5 pA; noncircular particles' shapes originate from STM feedback artifacts and nonideal geometry of the tip; (d) 0.5 ML, 1.8 V, 1 nA; (e) 1 ML, 1.55 V, 1 nA; (f) 14 ML, −1.0 V 0.5 nA.

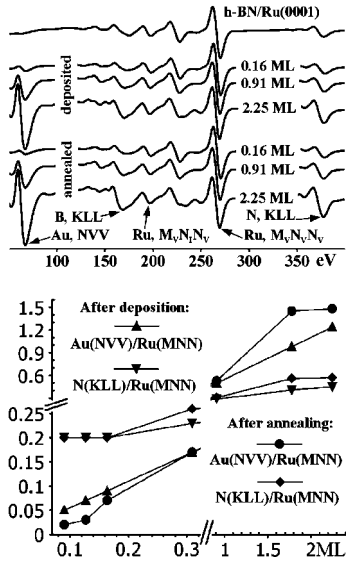

Figure 5. AES spectra of the pure h-BN/Ru(0001) and of the Au/h-BN/Ru(0001) for three particular Au coverages (RT deposition) and subsequent annealing at 1050 K. The chart shows the AES peak ratios of Ru (MNN, 273 eV), N (KLL, 379 eV), and Au (NVV, 69 eV) as a function of initially deposited Au coverage.

than 0.3 ML. Starting with an Au coverage of $\theta_{Au} = 0.3$ ML deposited at RT, we observe no decrease of Au_{NVV}/Ru_{MNN} ratio after annealing to 1050 K. For initial Au coverages larger than 1 ML there is even a significant increase of the Au_{NVV}/Ru_{MNN} ratio after 1050 K annealing. This is in line with Au penetration under the h-BN layer, where the lateral distribution of gold is more uniform, thereby reducing the Ru Auger signal more effectively.

The behavior of the N_{KLL}/Ru_{MNN} ratio is also in line with this interpretation. If Au is underneath the h-BN nanomesh then Au damps only the Auger electrons coming from Ru but not those from N, thus increasing the N_{KLL}/Ru_{MNN} ratio. The initial h-BN/Ru(0001) surface without Au is characterized by N_{KLL}/Ru_{MNN} ratio of 0.2 ± 0.02. At large Au coverages there are even higher than 0.2 N_{KLL}/Ru_{MNN} ratios just after Au deposition and before 1050 K annealing. This may indicate that some Au penetration underneath the h-BN may already take place at room temperature.

In concern for the chemical nature in which Au exists under the h-BN/Ru(0001), there are two possible alternatives. Gold may either form a pseudomorphic layer on Ru(0001) or Au forms a Au−Ru alloy under the h-BN nanomesh. It is known that gold does not grow in a pseudomorphic way on clean Ru(0001);[21] however, under a h-BN layer the energy balance may favor a pseudomorphic Au monolayer. A pseudomorphic Au film is required since the periodicity of the h-BN nanomesh on the islands is identical to that on Ru(0001). The existence of a h-BN nanomesh on the islands requires very specific properties of the supporting metal substrate such as the periodicity and the electronic structure. Among pure transition metals only Ru(0001) and Rh(111) are known to fulfill these requirements so far.[11,14,22] These specific conditions may be fulfilled by a pseudomorphic Au film on Ru(0001) or by a surface Au_xRu_y alloy. A differentiation between these models requires further detailed diffraction experiments and ab initio modeling and is beyond the scope of the present paper.

Deposition of a large amount of Au (such as 14 ML of initially deposited Au in Figure 2f) produces a continuous film of pure Au on top of Ru(0001) and underneath the h-BN nanomesh upon 1050 K annealing (Figure 4f). This is corroborated by the XPS data (Figure 6) for Au4f, B1s, and N1s emissions for initial $\theta_{Au} = 1$ ML and $\theta_{Au} = 14$ ML after Au deposition at RT and after subsequent annealing at 1050 K. For comparison we also present the same spectra taken on the pure

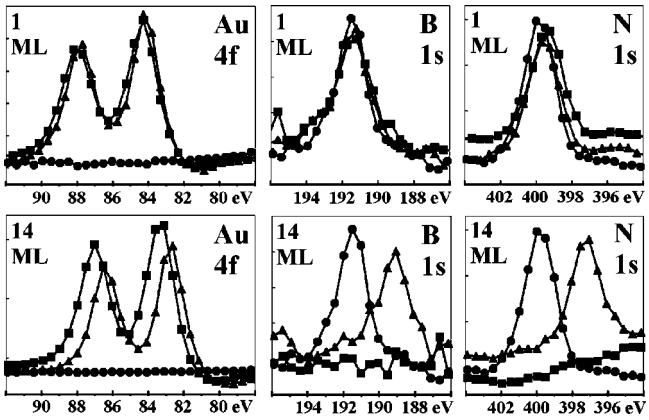

Figure 6. XPS of Au 4f, B 1s, and N 1s excited by Mg K_α radiation ($h\nu = 1253.6$ eV) for the two cases of 1 and 14 ML of Au initially deposited at room temperature. Horizontal axis: binding energy in eV relative to the Fermi edge. Vertical axis: intensity in arbitrary units. Squares: after deposition of Au onto the h-BN/Ru(0001) at RT. Triangles: after further annealing at 1050 K. For comparison, the pure h-BN/Ru(0001) surface is shown (circles).

h-BN/Ru(0001). After RT deposition of Au, the B1s and N1s emissions are completely suppressed by the as-deposited Au film of $\theta_{Au} = 14$ ML, while for $\theta_{Au} = 1$ ML this reduction in emission is negligible for N1s or at a noise level (B1s). After annealing the 14 ML Au film to 1050 K, the N1 and B1s emissions are almost restored. This observation supports a Au penetration below the h-BN. In the case of $\theta_{Au} = 14$ ML, the buried Au layer should act as a pure substrate (presumably Au(111) orientation), since no Au−Ru bulk alloy exists. As shown by DFT calculations, the h-BN monolayer on Au(111) is only weakly bound if calculated using WC or LDA functionals or even unbound if calculated with the PBE functional.[11] Thus, on Au(111) there is no strong modulation of interaction strength expected, which could produce the height modulation as in the h-BN nanomesh on Ru(0001). Therefore STM does not show a nanomesh type topography on a buried 14 ML Au film (Figure 4f).

In Figure 6 there are substantial shifts of Au4f, N1s, and B1s in the spectra toward lower binding energies upon annealing the $\theta_{Au} = 14$ ML film to 1050 K. These shifts are absent in the $\theta_{Au} = 1$ ML film, probably because the substrate on which the h-BN layer is resting possesses properties, which are rather close to those of Ru(0001) both before and after annealing. The B1s and N1s shifts seen for the 14 ML Au film after annealing in comparison with that of the pure h-BN nanomesh may be related to the varying bond strength of the h-BN layer to the underlying substrate, i.e., weakly bound/unbound in BN-Au vs strongly bound h-BN/Ru(0001) system. However, we believe that the B1s and N1s shifts of ∼2.5 eV are too large to be solely explained by the chemical binding arguments. For example, a similar comparison between the strongly chemisorbed h-BN/Ni(111) and only weakly chemisorbed h-BN/Cu(111),[23] showed no B1s shift and a modest −0.65 eV N1s shift.

Conclusions

In summary, we have performed an in-depth STM study of Au deposition on the h-BN/Ru(0001) nanomesh. As expected, the nanomesh serves as a scaffold for Au nanoparticles in that the Au particles nucleate exclusively in the pores (at least for low Au coverages). Besides Au nanoparticles, 2-dimensional aggregates of Au were created either on top of or below the h-BN layer, depending on the applied annealing temperature. Au tends to bury under the nanomesh on annealing to 1050 K if the total deposited Au amount is $\theta_{Au} > 0.3$ ML. Multilayers of deposited Au intercalate between Ru(0001) and the h-BN layer on annealing to 1050 K, forming presumably a Au(111)-oriented films and leading to the removal of nanostructuring of the h-BN overlayer due to the very week interaction between Au and h-BN.

Acknowledgment. We gratefully acknowledge the financial support from the European Union under Contract No. NMP4-CT-2004-013817 (Nanomesh). We are indebted to Hermann Sachdev for the supply of freshly synthesized borazine. We thank Thomas Greber for many enlightening discussions.

References and Notes

(1) (a) Haruta, M.; Yamada, N.; Kobayashi, T.; Iijima, S. *J. Catal.* **1989**, *115*, 301. (b) Haruta, M. *Gold Bull.* **2004**, *37*, 27.
(2) Chen, M. S.; Goodman, D. W. *Science* **2004**, *306*, 252.
(3) Valden, M.; Lai, X.; Goodman, D. W. *Science* **1998**, *281*, 1647.
(4) Cosandey, F.; Madey, T. *Surf. Rev. Lett.* **2001**, *8*, 73.
(5) Heiz, U.; Sanchez, A.; Abbet, S.; Schneider, W.-D. *Eur. Phys. J. D* **1999**, *9*, 35.
(6) Campbell, T. C.; Grant, A. W.; Starr, D. E.; Parker, S. C.; Bondzie, V. A. *Top. Catal.* **2001**, *14*, 43.
(7) Wang, J. G.; Hammer, B. *Phys. Rev. Lett.* **2006**, *97*, 136107.
(8) Wahlström, E.; Lopez, N.; Schaub, R.; Thostrup, P.; Rønnau, A.; Africh, C.; Lægsgaard, E.; Nørskov, J. K.; Besenbacher, F. *Phys. Rev. Lett.* **2003**, *90*, 026101.
(9) Corso, M.; Auwärter, W.; Muntwiler, M.; Tamai, A.; Greber, T.; Osterwalder, J. *Science* **2004**, *303*, 217.
(10) Goriachko, A.; He, Y.; Knapp, M.; Over, H.; Corso, M.; Brugger, T.; Berner, S.; Osterwalder, J.; Greber, T. *Langmuir Lett.* **2007**, *23*, 2928.
(11) Tran, F.; Laskowski, R.; Blaha, P.; Schwarz, K. *Phys. Rev. B* **2007**, *75*, 115131.
(12) PD Dr. Herman Sachdev, Anorganische Chemie, Universität des Saarlandes, Postfach 151150, D-66041 Saarbrücken, Germany. E-mail adress: h.sachdev@mx.uni-saarland.de.
(13) Gsell, M.; Jakob, P.; Menzel, D. *Science* **1998**, *289*, 717.
(14) Preobrajenski, A. B.; Vinogradow, A. S.; Ng, M. L.; Ćavar, E.; Westerström, R.; Mikkelsen, A.; Lundgren, E.; Mårtensson, N. *Phys. Rev. B* **2007**, *75*, 245412.
(15) Laskowski, R.; Blaha, P.; Gallauner, T.; Schwarz, K. *Phys. Rev. Lett.* **2007**, *98*, 106802.
(16) Berner, S.; Corso, M.; Widmer, R.; Groening, O.; Laskowski, R.; Blaha, P.; Schwarz, K.; Goriachko, A.; Over, H.; Gsell, S.; Schreck, M.; Sachdev, H.; Greber, T.; Osterwalder, J. *Angew. Chem., Int. Ed.* **2007**, *46*, 5115.
(17) Dil, H.; Lobo-checa, J.; Laskowski, R.; Blaha, P.; Berner, S.; Osterwalder, J.; Greber, T. *Science* **2008**, *319*, 1824.
(18) Auẅarter, W.; Muntwiler, M.; Greber, T.; Osterwalder, J. *Surf. Sci.* **2002**, *511*, 379.
(19) Harendt, C.; Christmann, K.; Hirschwald, W.; Vickerman, J. C. *Surf. Sci.* **1986**, *165*, 413.
(20) Besenbacher, F.; Chorkendorff, I.; Clausen, B. S.; Hammer, B.; Molenbroek, A. M.; Nørskov, J. K.; Stensgaard, I. *Science* **1998**, *279*, 1913.
(21) (a) Hwang, R. Q.; Behm, R. J. *J. Vac. Sci. Technol.* **1992**, *10*, 256. (b) Hwang, R. Q.; Schroeder, J.; Guenther, G.; Behm, R. J. *Phys. Rev. Lett.* **1991**, *67*, 3279.
(22) Preobrajenski, A. B.; Nesterov, M. A.; Ng, M. L.; Vinogradow, A. S.; Mårtensson, N. *Chem. Phys. Lett.* **2007**, *446*, 119.
(23) Preobrajenski, A. B.; Vinogradow, A. S.; Mårtensson, N. *Surf. Sci.* **2005**, *582*, 21.

JP7119608